Improved stability of a protein vaccine through elimination of a partially unfolded state

COLLEEN A. MCHUGH, RALPH F. TAMMARIELLO, CHARLES B. MILLARD, AND JOHN H. CARRA

United States Army Medical Research Institute of Infectious Diseases, Department of Cell Biology and Biochemistry, Frederick, Maryland 21702, USA

(RECEIVED May 28, 2004; FINAL REVISION June 29, 2004; ACCEPTED July 2, 2004)

Abstract

Ricin is a potent toxin presenting a threat as a biological weapon. The holotoxin consists of two disulfide-linked polypeptides: an enzymatically active A chain (RTA) and a galactose/*N*-acetylgalactosamine-binding B chain. Efforts to develop an inactivated version of the A chain as a vaccine have been hampered by limitations of stability and solubility. Previously, recombinant truncated versions of the 267-amino-acid A chain consisting of residues 1–33/44–198 or 1–198 were designed by protein engineering to overcome these limits and were shown to be effective and nontoxic as vaccines in mice. Herein we used CD, dynamic light scattering, fluorescence, and Fourier-transform infrared spectroscopy to examine the biophysical properties of these proteins. Although others have found that recombinant RTA (rRTA) adopts a partially unfolded, molten globule–like state at 45°C, rRTA 1–33/44–198 and 1–198 are significantly more thermostable, remaining completely folded at temperatures up to 53°C and 51°C, respectively. Deleting both an exposed loop region (amino acids 34–43) and the C-terminal domain (199–267) contributed to increased thermostability. We found that chemically induced denaturation of rRTA, but not the truncated variants, proceeds through at least a three-state mechanism. The intermediate state in rRTA unfolding has a hydrophobic core accessible to ANS and an unfolded C-terminal domain. Removing the C-terminal domain changed the mechanism of rRTA unfolding, eliminating a tendency to adopt a partially unfolded state. Our results support the conclusion that these derivatives are superior candidates for development as vaccines against ricin and suggest an approach of reduction to minimum essential domains for design of more thermostable recombinant antigens.

Keywords: protein folding; stability; ricin; vaccine

Ricin toxin is a lethal ribosome-inactivating protein found in the seeds of *Ricinus communis* (Lord et al. 1994; Olsnes and Kozlov 2001). No licensed vaccines or therapeutic measures are available. The holotoxin is made up of two polypeptides, A and B, linked by a disulfide bond. The ricin B chain binds to membrane oligosaccharides containing galactose or *N*-acetylgalactosamine and triggers endocytosis of the holotoxin. Inside the cell, ricin travels to the ER via retrograde transport, in which the disulfide bond between chains is reduced (Hazes and Read 1997; Lord and Roberts 1998). The A chain (Mlsna et al. 1993; Weston et al. 1994) then translocates to the cytosol, where it inactivates the 60S ribosomal subunit by removing a specific adenine base from 28S rRNA. One molecule of RTA in the cytosol is able to kill a cell by halting protein synthesis (Eiklid et al. 1980).

Recent threats of biological warfare and bioterrorism, combined with the widespread availability of castor beans, highlight the need for a safe and effective vaccine against ricin poisoning. However, earlier efforts to develop a recombinant protein vaccine encountered difficulties with limitations in solubility and stability.

Reprint requests to: John Carra, United States Army Medical Research Institute of Infectious Diseases, Department of Cell Biology and Biochemistry, 1425 Porter Street, Frederick, MD 21702, USA; e-mail: john.carra@det.amedd.army.mil; fax: (301) 619-2348.

Article published online ahead of print. Article and publication date are at http://www.proteinscience.org/cgi/doi/10.1110/ps.04897904.

Argent et al. (2000) reported that recombinant ricin A chain (rRTA) produced in bacteria is relatively unstable compared with a typical globular protein, adopting at 45°C a monomeric, partially unfolded, or "molten globule," state. These investigators proposed that such an intermediate exists in vivo during translocation of rRTA from the ER to the cytosol through cellular machinery for the recognition, export, and degradation of misfolded polypeptides. They also presented evidence that it refolds to an active form on contact with ribosomes in the cytosol.

Nontoxic derivatives of rRTA (267 aa) can elicit protective immunity, but the low thermostability of rRTA and its tendency to undergo partial unfolding are undesirable characteristics for a vaccine (Brandau et al. 2003). Several rRTA variants with point mutations in the active site have been investigated (Schlossman et al. 1989; Ready et al. 1991; Kim and Robertus 1992; Kim et al. 1992; Day et al. 1996), but the folding stabilities of these polypeptides have either not been reported or are equal to or less than that of rRTA itself. Additional substitution of residues implicated in vascular leak syndrome, observed when RTA is used in high doses as part of an immunotoxin, has been proposed (Smallshaw et al. 2002, 2003).

To overcome the limitations of rRTA, single-domain versions were designed by Olson et al. (2003, 2004) to be more stable and soluble antigenic platforms (Fig. 1). rRTA 1–198 lacks the C-terminal domain (residues 199 to 267), whereas rRTA 1–33/44–198 has an external loop region (residues 34–43) deleted. Residues 95–110 (Lebeda and Olson 1999) and 161–175 (Castelleti et al. 2004) comprising major neutralizing B-cell epitopes were retained in both constructs. Removing the C-terminal domain abolished the toxic *N*-glycosidase activity of RTA, whereas deleting residues 34–43 further reduced its size and eliminated a potentially disordered region. Intramuscular vaccination with rRTA 1–33/44–198 or 1–198 effectively protected mice challenged by injection or aerosol with ricin toxin (Olson et al. 2004).

Herein we investigated the folding of recombinant and natural RTA, and two engineered variants created as potential vaccines. We found that rRTA 1–33/44–198 and 1–198 had improved stabilities versus temperature and denaturant, and we relate these properties to the absence of an intermediate state in unfolding observed with the parent molecule rRTA.

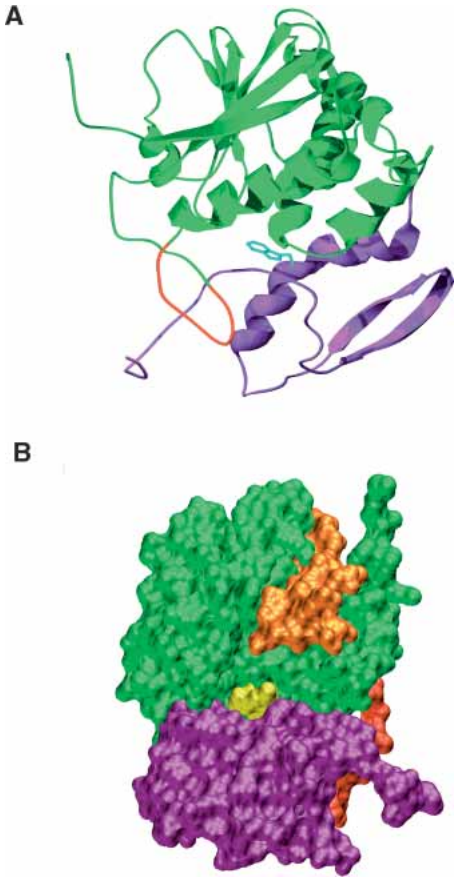

Figure 1. rRTA structure. (*A*) The N-terminal domain is shown in green, loop (amino acids 34–43) in red; C-terminal domain (amino acids 199–267), in purple; and the single tryptophan (amino acids 211), in cyan (1rtc.pdb; Mlsna et al. 1993). (*B*) Surface model of the opposite side of the molecule. Active site residues E177 and R180 are shown in yellow, and a neutralizing epitope (amino acids 95–110) in orange. Figures drawn with PyMol (Delano Scientific).

Results

The rRTA derivatives are appropriately folded and have increased thermostability

To check if removing amino acids in the 1–33/44–198 and 1–198 proteins perturbed overall folding, we examined their far-UV CD spectra (Fig. 2A). The spectra of the two mutants were nearly superimposable and only slightly different from those of rRTA and natural glycosylated A chain (nRTA), indicating they have similar secondary structure contents. This result is consistent with the percentages of α-helix and β-sheet predicted assuming conservation in the mutants from the known structure of rRTA (Mlsna et al. 1993). rRTA contains 32% α-helix and 16% β-sheet, whereas removing residues 34–43 and 199–267 from the same structure would yield 36% α-helix and 17% β-sheet. The small increase in α-helicity in the mutants versus rRTA was reflected in slightly greater ellipticities at 222 nm, whereas their Y-intercept at a shorter wavelength is consistent with a minor reduction in disordered regions. The large deletions in these derivatives did not, however, appear to induce major structural changes in the remainder of the protein.

To probe tertiary structure of the proteins, we examined near-UV CD spectra (Fig. 2B). The spectra of rRTA 1–33/44–198 and rRTA 1–198 were nearly identical, with a major

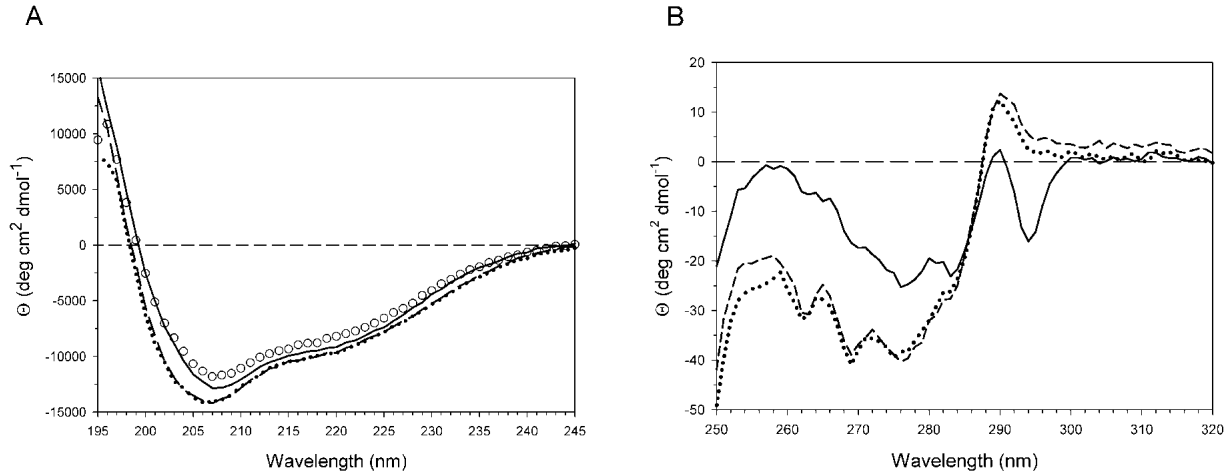

Figure 2. CD spectra. (*A*) Far-UV spectra at 5°C of rRTA (solid line), rRTA 1–33/44–198 (dashed line), rRTA 1–198 (dotted line), and nRTA (circles). (*B*) Near-UV CD spectra at 5°C of rRTA (solid line), rRTA 1–33/44–198 (dashed line), and rRTA 1–198 (dotted line).

peak near 288 nm. Near-UV CD spectra of proteins reflect asymmetry in the electronic environment of aromatic side-chains. Strongly featured spectra indicate native-like residue packing, in contrast to the absence of signal seen with molten globule species. The negative peak found for rRTA at 294 nm, a wavelength in which tyrosine does not absorb strongly, was absent in the truncated derivatives. This was presumably due to removal of the single tryptophan at position 211 with deletion of the C-terminal domain.

Figure 3 shows deuterated Fourier-transform infrared spectroscopy (FTIR) spectra in the amide I′ region for rRTA versus rRTA 1–33/44–198. The shapes of these two spectra and that of rRTA 1–198 (data not shown) are very similar, in agreement with the conclusion from CD spectra that secondary structure content was conserved in these derivatives. Spectral deconvolution was not attempted due to uncertainties in this approach and the observation that overall secondary structure content was little altered by the deletions. Conservation of structure is an important consideration for correct presentation of neutralizing epitopes, which for residues 95–110 was predicted to be conformational (Lebeda and Olson 1999).

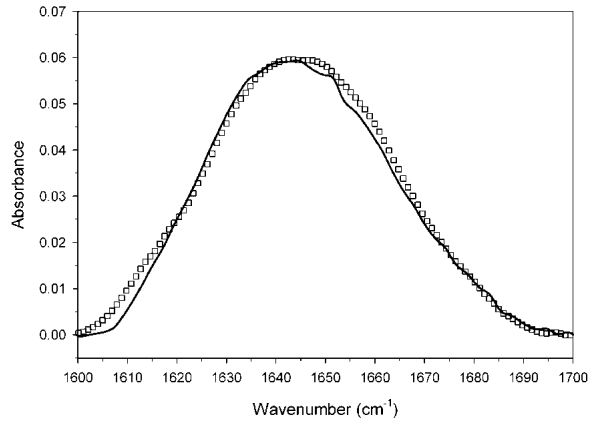

Figure 3. FTIR spectra at 25°C in the amide I′ region: rRTA (squares) and rRTA 1–33/44–198 (solid line). Measurements were normalized to the same absorbance at 1640 cm^{-1} to facilitate comparison.

We then assayed the relative stabilities of these proteins by using thermal melting followed by ellipticity at 205 nm (Fig. 4), the wavelength at which the signal change on unfolding was maximal. Denaturation of rRTA began at 47°C, in fair agreement with the results of Argent et al. (2000), whereas rRTA 1–33/44–198 started to denature only at 53°C (Table 1). rRTA 1–198 was intermediate between the two, with a denaturational onset of 51°C. Glycosylation of RTA in the plant-derived protein (nRTA) had little effect on the onset of thermal denaturation, although the melting curve of this protein was broader and more symmetric. Thermal denaturation of rRTA and its derivatives was irreversible and scan-rate dependent and resulted in precipitation as judged by an increase in turbidity. This behavior precluded calculation of the ΔG of folding. Therefore, we use the temperature of onset of denaturation, defined as the point of 5% signal change, as a marker of relative thermal stability. An increase in β-sheet content in the heat-denatured state was observed by FTIR and CD for all the proteins (data not shown).

Improved resistance to aggregation and precipitation

Dynamic light-scattering measurements (Table 2) showed that rRTA and its derivatives 1–33/44–198 and 1–198 exist as monodisperse monomers at 0.8 mg/mL in PBS at 25°C. The hydrodynamic radii measured were within 10% of those expected for monomer species.

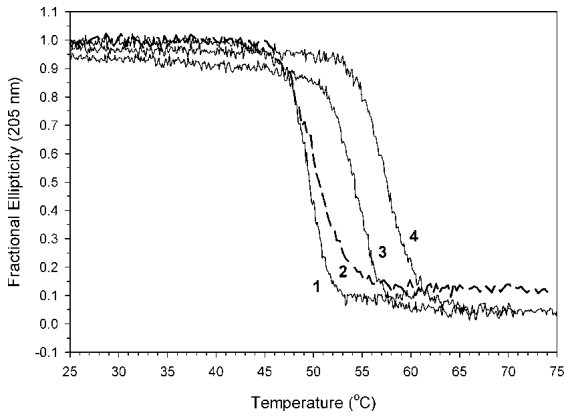

Figure 4. Thermal denaturation followed by ellipticity at 205 nm: 1, rRTA; 2, nRTA; 3, rRTA 1–198; and 4, rRTA 1–33/44–198.

rRTA 1–33/44–198 and rRTA 1–198 were also more resistant than rRTA to aggregation and precipitation induced by extended incubation at physiological temperature. Proteins were incubated for extended times at 37°C in PBS, and the percentage remaining soluble after centrifugation was measured. rRTA 1–33/44–198 mostly persisted in solution in this assay, whereas rRTA was almost entirely found in the insoluble pellet. Only 6% of rRTA remained in solution after incubation after 106 h (Table 1), whereas 25% of rRTA 1–198 and 58% of rRTA 1–33/44–198 remained soluble. A greater fraction of nRTA (31% vs. 6%) than rRTA remained soluble. This finding is consistent with glycosylation reducing the tendency of the protein to irreversibly aggregate and precipitate. Analysis by SDS-PAGE (data not shown) detected no proteolytically cleaved products for these proteins in either the soluble or insoluble fractions.

Sensitivity to proteolysis

Treating rRTA, rRTA 1–198, and rRTA 1–33/44–198 with thermolysin revealed differences in their sensitivities to digestion. Previously, rRTA was highly resistant to proteinase K digestion and able to survive treatment with 1 mg/mL protease (Walker et al. 1996). We found that rRTA was also quite resistant to thermolysin cleavage (Fig. 5). Some digestion of rRTA did occur after 60 min of incubation with thermolysin, but approximately half of the protein was intact. In contrast, all but a small fraction of rRTA 1–198 was digested to small fragments after 10 min. The increased susceptibility of rRTA 1–198 to thermolysin digestion was most likely due to exposure and disordering of loop residues 34–44 as a result of truncation of the C-terminal domain. In the structure of rRTA (Fig. 1), the C-terminal domain is packed against this loop, protecting it from a cleavage event rapidly followed by further degradation.

For rRTA 1–33/44–198, a short peptide was cleaved off upon protease treatment, but the majority of the protein persisted as a more resistant core. Analysis by mass spectroscopy indicated that cleavage occurred after tyrosine 183, at the beginning of the final α-helix of the N-terminal domain. The short loop preceding this helix makes contacts to residues 251–253 in the C-terminal domain of RTA. Truncation at residue 198 in the mutant protein may have increased chain mobility and proteolytic sensitivity near residue 183, although we found this sensitivity did not present a problem for protein expression, isolation, and storage.

Table 1. *Parameters of denaturation of RTA proteins*

Protein	T_d[a]	C_m[b]	% soluble[c]
rRTA	46.6 ± 0.1	1.56 ± 0.022	6 ± 3.4
rRTA 1–198	50.8 ± 0.5	2.29 ± 0.004	25 ± 4.5
rRTA 1–33/44–198	53.1 ± 0.1	2.53 ± 0.041	58 ± 1.3
nRTA	45.6 ± 0.1	1.39 ± 0.020	31 ± 7.2

[a] Temperature of onset of denaturation in thermal melting (°C) as monitored by CD at 205 nm. T_d was taken as the point at which the signal had diverged from that of the native state by 5%. Results are the average and standard error of three measurements.
[b] The midpoint concentration of guanidine-HCl denaturation in molar, as measured by CD at 225 nm.
[c] The percentage of protein remaining soluble after incubation for 106 h at 37°C.

Table 2. *Dynamic light-scattering measurements*

Protein	R_h[a]	Hydrodynamic MW_r[b]	Actual MW_r[c]
rRTA	2.53	29.5×10^3	30.0×10^3
rRTA 1–198	2.16	20.4×10^3	22.5×10^3
rRTA 1–33/44–198	2.11	19.3×10^3	21.3×10^3

[a] The hydrodynamic radius of the protein in solution as measured by DLS, in nanometers.
[b] Molecular weight calculates from R_h.
[c] Molecular weight of a monomer from the protein sequence.

Unfolding intermediate of rRTA not present in the mutants

The origin of the increased thermostabilities of the rRTA derivatives was explored by examining more closely their mechanisms of denaturation. The proteins were unfolded by titration with guanidine-HCl, whereas circular dichroism (CD) and fluorescence emission were measured simultaneously. Relative changes in ellipticity at 225 nm, and intrinsic fluorescence emission are plotted as functions of denaturant concentration in Figure 6A. Also plotted is fluorescence from the hydrophobic dye 8-anilino-1-naphthalenesulfonate (ANS), added to the protein solution in a separate experiment.

The unfolding of rRTA was more complicated than a simple two-state process, as can be seen by comparing the

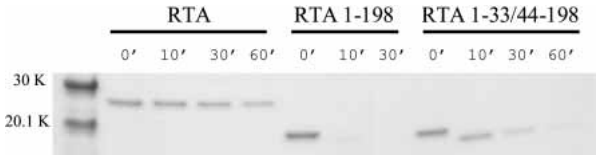

Figure 5. Digestion of rRTA, rRTA 1–198, or rRTA 1–33/44–198 by thermolysin at 37°C for the indicated times in minutes. Zero-minute samples were incubated without protease for 1 h at 37°C as undigested controls.

data for tryptophan emission only (excited selectively at 295 nm and monitored at 320 nm) versus emission at 303 nm with excitation at 280 nm, which included components from excitation of both tyrosine and tryptophan. rRTA contains 14 tyrosines, 12 of which are in the N-terminal domain, and one tryptophan at position 211 in the C-terminal domain. Tryptophan 211 had its fluorescence quenched in a transition that finished by 1.8 M guanidine-HCl, whereas the emission at 303 nm first decreased until 1.8 M denaturant and then increased in a second transition. Fluorescence from ANS, which has an affinity for partially folded states of proteins (Fink 1995), increased to a maximum at 1.9 M guanidine-HCl and then decreased more slowly. The change in CD signal mostly paralleled the change in tryptophan emission, with some indication of a second broader transition.

Figure 6B presents the variation in fluorescence emission spectra of rRTA as a function of guanidine-HCl concentration. The spectra can be seen to shift from a maximum at 328 nm to one near 303 nm, reflecting the quenching of tryptophan and subsequent increase of tyrosine fluorescence as denaturation proceeds in two phases.

Judging from these data, denaturation of rRTA is at least a three-state process, including an intermediate state in which Trp 211 is exposed to solvent. Residual structure remains in this form, providing an accessible hydrophobic region able to bind ANS, with a resultant increase in the fluorescence of the dye. With further increase of guanidine-HCl concentration from 1.8 M, this residual structure was disrupted, yielding a small increase in tyrosine fluorescence and a decrease in ANS emission.

By using the same probes, we also followed the denaturation of rRTA 1–33/44–198 and rRTA 1–198 (Fig. 6C,D). These derivatives have the 12 tyrosines of the RTA N-terminal domain and no tryptophan. Their tyrosine fluorescence increased 1.75-fold with denaturation, which can be attributed to a relief from quenching interactions present in the native state. The change in tyrosine emission paralleled the change in CD, whereas fluorescence from ANS decreased gradually up to 2 M guanidine-HCl, but changed little through the region of protein unfolding. Neither probe gave clear signs of an intermediate state as with wild-type rRTA.

The magnitude of the normalized increase in fluorescence emission at 303 nm in the second phase of denaturation of rRTA was not as great as for the two mutant derivatives, due to the significant contribution of tryptophan 211 in rRTA in the folded state. ANS did bind to the folded states of both rRTA 1–33/44–198 and rRTA 1–198, but the decrease in ANS fluorescence observed at low guanidine-HCl concentrations suggests that this was due to electrostatic interactions of the sulfate group of ANS, which weakened as ionic strength increased. ANS also binds weakly to the native state of wild-type rRTA (Houston 1980).

Unfolding of rRTA 1–33/44–198 followed by CD had a denaturant midpoint concentration of 2.5 M guanidine-HCl (Table 1), whereas the midpoint of rRTA by this criterion was only 1.6 M, in fair agreement with the results of Bushueva and Tonevitsky (1987). rRTA 1–33/44–198 was therefore significantly more stable to solvent denaturation than was rRTA, in accord with results from thermal melting. rRTA 1–198 was slightly less stable than 1–33/44–198, with a midpoint of 2.3 M guanidine-HCl. Similar results to those for rRTA were obtained for plant-derived nRTA, with a midpoint denaturation concentration of 1.4 M guanidine-HCl.

Because the irreversibility of rRTA unfolding (Argent et al. 2000) precludes detailed thermodynamic analysis, we do not present ΔG values for folding. Nevertheless, the CD and fluorescence data for rRTA 1–33/44–198 or rRTA 1–198 (Fig. 6C) could be well fit simultaneously by nonlinear regression to a two-state model of unfolding for each protein (Pace et al. 1989). The CD and fluorescence signal changes were clearly coincident, following the same transition between states. Coincidence of two such observations is a commonly accepted criterion for the existence of only two states, the native and denatured, without the presence of an intermediate. Unfolding data for rRTA in contrast could not be fit to a two-state model, due to the more complex nature of the process.

Discussion

Unfolding mechanisms and changes in stability

Detailed interpretation of denaturation curves is difficult for an irreversibly unfolding protein. However, given that almost all pharmaceutically relevant proteins behave in this way, and that folding stability is an important consideration for their production, it is worthwhile to try to derive some insight into the properties of the rRTA derivatives from a consideration of protein structure and unfolding mechanisms.

The absence for rRTA 1–33/44–198 and rRTA 1–198 of a partially unfolded intermediate strongly suggests that the smaller C-terminal domain, deleted in these mutants, is relatively unstable and responsible for the early unfolding transition of rRTA. This point is also supported by comparison of unfolding transitions monitored by multiple spectro-

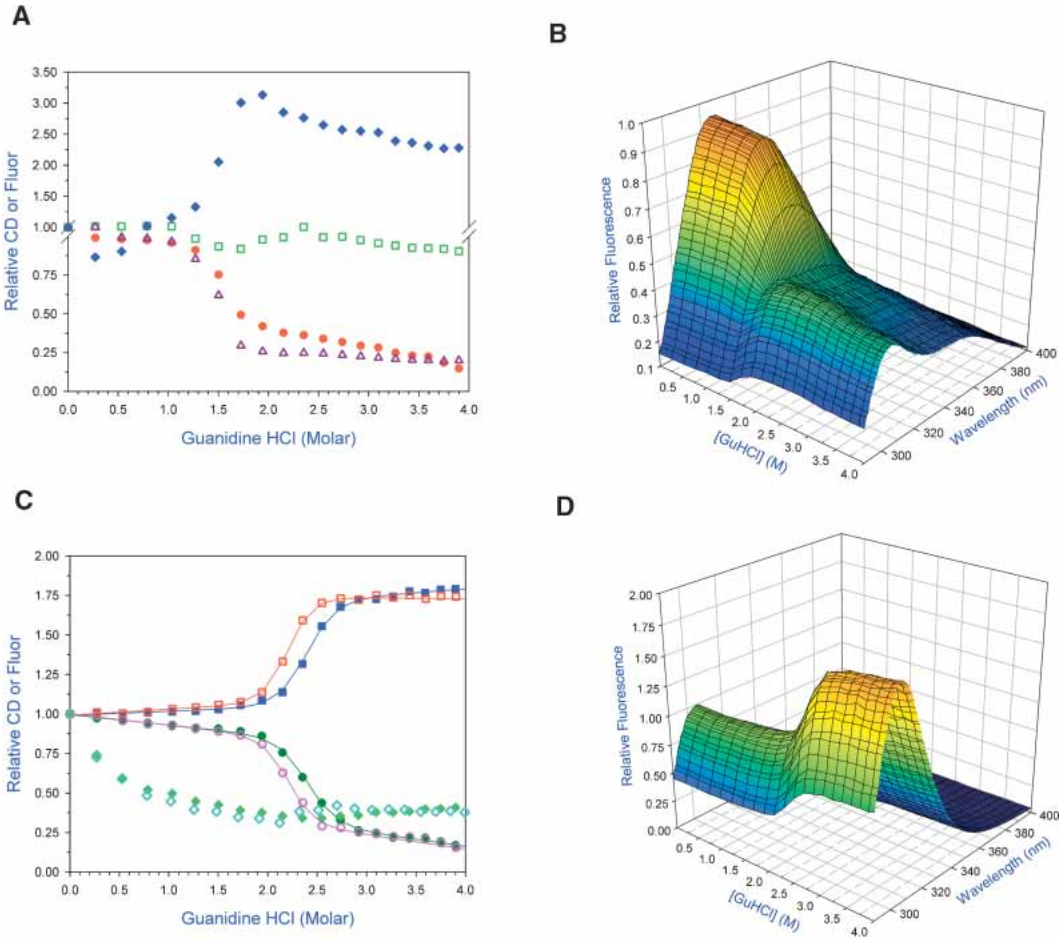

Figure 6. Chemical denaturation followed by CD and fluorescence. (*A*) Denaturation of rRTA by guanidine-HCl was followed in one experiment by CD at 225 nm, intrinsic fluorescence emission at 303 nm with excitation at 280 nm, and emission at 320 nm with excitation at 295 nm. In a separate experiment, fluorescence from 50 μm ANS at 480 nm was observed in the presence of the protein: CD (circles), fluorescence with excitation at 280 nm and emission at 303 nm (squares), fluorescence with excitation at 295 nm and emission at 320 nm (triangles), and ANS fluorescence (diamonds). (*B*) Fluorescence emission spectra of rRTA as a function of guanidine-HCl concentration, with excitation at 280 nm. (*C*) Denaturation of rRTA 1–33/44–198 (filled symbols, as in *A*) and rRTA 1–198 (unfilled symbols). Excitation at 295 nm was not done due to the absence of tryptophan. Solid lines indicate fitting of the data to a two-state model of unfolding. (*D*) Fluorescence emission spectra for rRTA 1–33/44–198, with excitation at 280 nm.

scopic probes, including a single tryptophan residue present in the C-terminal domain.

The cause of the increases in denaturational temperature and guanidine-HCl midpoint when the C-terminal domain of rRTA was truncated may be understood in terms of a change in mechanism of unfolding from multistate to two-state. The large active-site cleft in the structure of rRTA apparently limited interdomain contacts and resulted in partial independence of the C-terminal domain as a folding unit (Fig. 7). Transformation to a partially folded intermediate upon early unfolding of this domain effectively limited the stability of wild-type rRTA but not the two mutant derivatives studied.

Our evidence suggests that the intermediate in unfolding of rRTA is better described as containing a partially folded N-terminal domain and an unfolded C-terminal domain, rather than as a uniformly altered structure or molten globule (Carra and Privalov 1995; Ptitsyn 1995). The cooperativity of unfolding of the intermediate state of rRTA is relatively low, consistent with some disruption of internal packing of the core of the protein having occurred in that state. However, we did observe the process clearly in changes in ANS and tyrosine fluorescence (Fig. 6A,B). It is likely that unfolding of the C-terminal domain is an essential step in translocation of RTA from the ER to the cytosol (Chaddock et al. 1995; Beaumelle et al. 1997; Argent et al. 2000; Day et al. 2002); therefore, the low conformational stability of this region may not be coincidental but a critical factor in its function.

Removing the loop residues 33–44 and the C-terminal domain both added to the apparent stabilities of the trun-

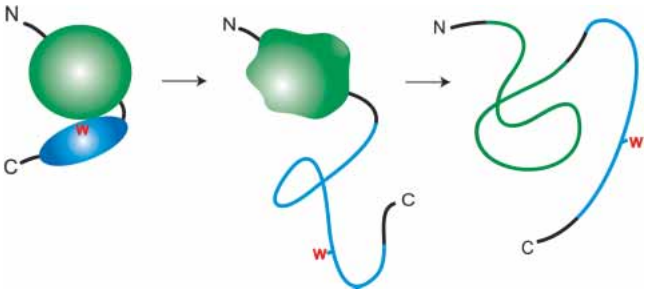

Figure 7. Unfolding model for RTA showing an intermediate state with a partially folded N-terminal domain.

cated proteins, with the latter making the larger contribution. Reducing the size of surface loops is expected, in general, to stabilize proteins by decreasing the entropic cost of loop closure during folding (Chan and Dill 1988).

We found that glycosylation of RTA in its natural form did not significantly alter the secondary structure or denaturational temperature of the protein, but decreased aggregation during thermal melting and extended incubation experiments. Glycosylation has been shown to reduce the aggregation of other denatured proteins (Wang et al. 1996). Preventing association of misfolded states in vivo may be a major benefit of this modification.

Implications for vaccine design

In general, the native state of a protein is only as stable as the energetic difference to the nearest accessible nonnative state. "Negative design" (Hecht et al. 1990) against nonnative states is therefore an important consideration for protein stability. In this case, a more thermostable protein was made by removing C-terminal domain residues that contributed to the adoption of a partly folded state. Deleting the C-terminal domain also eliminated toxic enzymatic activity by removing residues crucial to binding of substrate (Olson and Cuff 1999). A further improvement to the 1–198 construct was made by removing a newly protease-sensitive exposed loop, residues 34–43. The design of more stable proteins for use as antigens is in some ways a simpler problem than the design of thermostable enzymes because maintenance of enzymatic activity is unnecessary or, in the case of toxins, undesirable.

The toxicological and immunological properties (Olson et al. 2004) of the rRTA derivatives 1–33/44–198 and 1–198, along with the biophysical characteristics described here, indicate that they represent a significant advance over other ricin vaccine candidates. The engineered rRTA derivatives have high solubility and exist in solution as discrete monomers, unlike chemically modified RTA toxoids, which display pronounced aggregation (Thorpe et al. 1985). Their increased thermostability also confers advantages for vaccine production, formulation, and storage (Brandau et al. 2003).

Currently, a major goal in vaccine design is to create vaccines that do not require continuous refrigeration (the "cold chain"), or lyophilization with stabilizing agents. Our results suggest that the reduction of protein subunits to a minimum essential domain containing a neutralizing epitope should be tested on other antigens as a strategy to approach that goal.

Materials and methods

Protein preparation

The rRTA derivative rRTA 1–198 was genetically deleted of residues 199–267, whereas in rRTA 1–33/44–198, residues 34–43 were also removed (Olson et al. 2003). For expression, clones in a pET24 vector were introduced into *Escherichia coli* BL21(DE3) cells and grown in TB medium with 50 μg/mL kanamycin at 37°C. Cultures were induced in log phase growth with 1 mM IPTG and grown overnight at 25°C. Cells were lysed by using a microfluidizer (Microfluidics M-110Y) in 50 mM sodium phosphate and 2 mM EDTA (pH 7.3). The soluble fraction of the lysate was passed through a Pharmacia Mono Q 10/10 column, and the flow-through dialyzed against 50 mM MES and 2 mM EDTA buffer (pH 6.0). This was applied to a Mono S 5/5 column and eluted with a sodium chloride gradient. Fractions were analyzed by SDS-PAGE for purity, which was estimated to be >98%. The method of Gill and von Hippel (1989) was used to calculate an A_{280} (1 mg/mL) of 0.721 for rRTA 1–33/44–198, 0.686 for rRTA 1–198, and 0.789 for rRTA. The proteins were dialyzed into PBS buffer, which was used in all experiments. Natural glycosylated RTA from *R. communis* was obtained from Vector Laboratories.

Dynamic light scattering

Dynamic laser light-scattering measurements were made with a Dyna-Pro MS800 instrument (Protein Solutions, Inc.) on samples at 25°C in PBS buffer. The Dynamics software package provided with the instrument was used to calculate hydrodynamic molecular weights from a standard curve for small globular proteins. Results for rRTA and its derivatives indicated monodispersity. Protein solutions at 0.8 mg/mL were passed through a 0.02-μM filter to remove particulates before use.

CD and fluorescence

Far-UV CD spectra on protein solutions at 0.2 mg/mL, in PBS buffer at 5°C, were taken with a Jasco-810 spectropolarimeter and 1-mm pathlength cell. Four scans were averaged, and data were not smoothed. Near-UV measurements were done at 0.8 mg/mL, 1-cm pathlength and 5°C. In thermal melts, heating was done at 1 K/min with a Peltier temperature controller. In guanidine-HCl titration experiments, CD and fluorescence emission data were collected by using an automatic titrator and a fluorescence detector at a right angle to the excitation beam. Guanidine-HCl was mixed into a 0.2 mg/mL protein solution at 25°C in PBS buffer. Concentrations of guanidine-HCl solutions were measured with a refractometer (Nozaki 1972). Intrinsic fluorescence emission spectra were collected for each injection with excitation at 280 and 295 nm, as well as the ellipticity at 225 nm. The excitation bandwidth was 3 nm. In ANS-containing experiments, fluorescence emission at 480 nm from 50 μm ANS was measured with excitation at 380 nm.

Fourier-transform infrared spectroscopy

FTIR measurements were obtained with 20μg of protein by using horizontal attenuated total reflectance on a thermally controlled 45° angle ZnSe crystal with 25 internal reflections (PikeTech) at 25°C. Samples were deuterated to reduce absorbance in the amide I region from liquid water. Hydrogen/deuterium exchange was accomplished by flowing D_2O-saturated N_2 gas over a sample dried down on the crystal (Goormaghtigh et al. 1999); 250 scans were taken at 2 cm^{-1} resolution. The contribution of residual water vapor to the spectra was manually subtracted.

Protein stability versus incubation at 37°C

Protein samples at 0.2 mg/mL in PBS were incubated at 37°C for up to 106 h, in the presence of 2 mM DTT to prevent disulfide-bond formation. The solution was then centrifuged to pellet insoluble material. Protein concentration in the soluble fraction was measured by Bio-Rad protein dye assay.

Protease digestion

rRTA, rRTA 1–198, or rRTA 1–33/44–198 at 0.2 mg/mL in PBS was incubated at 37°C with 0.02 mg/mL thermolysin. Aliquots of protein were removed after 10, 30, and 60 min of incubation. The reactions were quenched with 10 mM EDTA and samples analyzed by SDS-PAGE.

Acknowledgments

We gratefully acknowledge the contributions of Rowena Schokman to this research project. Mass spectroscopy was performed by Ernst Brueggemann in the laboratory of Dr. Harry Hines. Opinions, interpretations, conclusions, and recommendations are those of the authors and are not necessarily endorsed by the US Army.

The publication costs of this article were defrayed in part by payment of page charges. This article must therefore be hereby marked "advertisement" in accordance with 18 USC section 1734 solely to indicate this fact.

References

Argent, R.H., Parrott, A.M., Day, P.J., Roberts, L.M., Stockley, P.G., Lord, J.M., and Radford, S.E. 2000. Ribosome-mediated folding of partially unfolded ricin A-chain. *J. Biol. Chem.* **275:** 9263–9269.

Beaumelle, B., Taupiac, M.P., Lord, J.M., and Roberts, L.M. 1997. Ricin A chain can transport unfolded dihydrofolate reductase into the cytosol. *J. Biol. Chem.* **272:** 22097–22102.

Brandau, D.T., Jones, L.S., Wiethoff, C.M., Rexroad, J., and Middaugh, C.R. 2003. Thermal stability of vaccines. *J. Pharm. Sci.* **92:** 106–119.

Bushueva, T.L. and Tonevitsky, A.G. 1987. The effect of pH on the conformation and stability of the structure of plant toxin: Ricin. *FEBS Lett.* **215:** 155–159.

Carra, J.H. and Privalov, P.L. 1995. Energetics of denaturation and *m* values of staphylococcal nuclease mutants. *Biochemistry* **34:** 2034–2041.

Castelletti, D., Fracasso, G., Righetti, S., Tridente, G., Schnell, R., Engert, A., and Colombatti, M. 2004. A dominant linear B-cell epitope of ricin A-chain is the target of a neutralizing antibody reponse in Hodgkin's lymphoma patients treated with an anti-CD25 immunotoxin. *Clin. Exp. Immunol.* **136:** 365–372.

Chaddock, J.A., Roberts, L.M., Jungnickel, B., and Lord, J.M. 1995. A hydrophobic region of ricin A chain which may have a role in membrane translocation can function as an efficient noncleaved signal peptide. *Biochem. Biophys. Res. Comm.* **217:** 68–73.

Chan, H.S. and Dill, K.A. 1988. Intrachain loops in polymers. *J. Chem. Phys.* **90:** 492–509.

Day, P.J., Ernst, S.R., Frankel, A.E., Monzingo, A.F., Pascal, J.M., Molina-Svinth, M.C., and Robertus, J.D. 1996. Structure and activity of an active site substitution of ricin A chain. *Biochemistry* **35:** 11098–11103.

Day, P.J., Pinheiro, T.J.T., Roberts, L.M., and Lord, J.M. 2002. Binding of ricin A-chain to negatively charged phospholipid vesicles leads to protein structural changes and destabilizes the bilayer. *Biochemistry* **41:** 2836–2843.

Eiklid, K., Olsnes, S., and Pihl, A. 1980. Entry of lethal doses of abrin, ricin and modeccin into the cytosol of HeLa cells. *Exp. Cell. Res.* **126:** 321–326.

Fink, A.L. 1995. Compact intermediate states in protein folding. *Annu. Rev. Biophys. Biomol. Struct.* **24:** 495–522.

Gill, S.C. and von Hippel, P.H. 1989. Calculation of protein extinction coefficients from amino acid sequence data. *Anal. Biochem.* **182:** 319–326.

Goormaghtigh, E., Raussens, V., and Ruysschaert, J.-M. 1999. Attenuated total reflection infrared spectroscopy of proteins and lipids in biological membranes. *Biochim. Biophys. Acta* **1422:** 105–185.

Hazes, B. and Read, R.J. 1997. Accumulating evidence suggests that several AB-toxins subvert the endoplasmic reticulum-associated protein degradation pathway to enter target cells. *Biochemistry* **36:** 11051–11054.

Hecht, M.H., Richardson, J.S., Richardson, D.C., and Ogden, R.C. 1990. De novo design, expression, and characterization of Felix: A four-helix bundle protein of native-like sequence. *Science* **249:** 884–891.

Houston, L.L. 1980. Differential fluorescence enhancement of 8-anilino-1-napthalene sulfonic acid by ricin A and B chains. *Biochem. Biophys. Res. Comm.* **92:** 319–326.

Kim, Y. and Robertus, J.D. 1992. Analysis of several key active site residues of ricin A chain by mutagenesis and X-ray crystallography. *Protein Eng.* **5:** 775–779.

Kim, Y., Mlsna, D., Monzingo, A.F., Ready, M.P., Frankel, A., and Robertus, J.D. 1992. Structure of a ricin mutant showing rescue of activity by a noncatlytic residue. *Biochemistry* **31:** 3294–3296.

Lebeda, F.J. and Olson, M.A. 1999. Prediction of a conserved, neutralizing epitope in ribosome-inactivating proteins. *Int. J. Biol. Macromol.* **24:** 19–26.

Lord, J.M. and Roberts, L.M. 1998. Toxin entry: Retrograde transport through the secretory pathway. *J. Cell Biol.* **140:** 733–736.

Lord, J.M., Roberts, L.M., and Robertus, J.D. 1994. Ricin: Structure, mode of action, and some current applications. *FASEB J.* **8:** 201–208.

Mlsna, D., Monzingo, A.F., Katzin, B.J., Ernst, S., and Robertus, J.D. 1993. Structure of recombinant ricin A chain at 2.3 Å. *Protein Sci.* **2:** 429–435.

Nozaki, Y. 1972. The preparation of guanidine hydrochloride. In *Methods in Enzymology*, Vol. 26, pp. 43–50.

Olsnes, S. and Kozlov, J.V. 2001. Ricin. *Toxicon* **39:** 1723–1728.

Olson, M.A. and Cuff, L. 1999. Free energy determinants of binding the rRNA substrate and small ligands to ricin A-chain. *Biophys. J.* **76:** 29–39.

Olson, M.A., Millard, C.B., Byrne, M.P., Wannemacher, R.W., and LeClaire, R.D. 2003. Ricin vaccine. U.S. Patent App. 20030181665.

Olson, M.A., Carra, J.H., Roxas-Duncan, V., Wannemacher, R.W., Smith, L.A., and Millard, C.B. 2004. Finding a new vaccine in the ricin fold. *Protein Eng. Des. Sel.* **17:** 391–397.

Pace, C., Shirley, B., and Thomson, J. 1989. Measuring the conformational stability of a protein. In *Protein structure: A practical approach* (ed. T.E. Creighton), pp. 311–330. IRL Press, Oxford.

Ptitsyn, O.B. 1995. How the molten globule became. *Trends Biochem. Sci.* **20:** 376–379.

Ready, M.P., Kim, Y., and Robertus, J.D. 1991. Site-directed mutagenesis of ricin A-chain and implications for the mechanism of action. *Proteins* **10:** 270–278.

Schlossman, D., Withers, D., Welsh, P., Alexander, A., Robertus, J., and Frankel, A. 1989. Role of glutamic acid 177 of the ricin toxin A chain in enzymatic inactivation of ribosomes. *Mol. Cell. Biol.* **9:** 5012–5021.

Smallshaw, J.E., Firan, A., Fulmer, J.R., Ruback, S.L., Ghetie, V., and Vitetta, E.S. 2002. A novel recombinant vaccine which protects mice against ricin intoxication. *Vaccine* **20:** 3422–3427.

Smallshaw, J.E., Ghetie, V., Rizo, J., Fulmer, J.R., Trahan, L.L., Ghetie, M.A., and Vitetta, E.S. 2003. Genetic engineering of an immunotoxin to eliminate pulmonary vascular leak in mice. *Nat. Biotech.* **21:** 372–374.

Thorpe, P.E., Detre, S.I., Foxwell, B.M., Brown, A.N., Skilleter, D.N., Wilson, G., Forrester, J.A., and Stirpe, F. 1985. Modification of the carbohydrate in ricin with metaperiodate-cyanoborohydride mixtures: Effects on toxicity and in vivo distribution. *Eur. J. Biochem.* **147:** 197–206.

Walker, D., Chaddock, A.M., Chaddock, J.A., Roberts, L.M., Lord, J.M., and Robinson, C. 1996. Ricin A chain fused to a chloroplast-targeting signal is unfolded on the chloroplast surface prior to import across the envelope membranes. *J. Biol. Chem.* **271:** 4082–4085.

Wang, C., Eufemi, M., Turano, C., and Giartosio, A. 1996. Influence of the carbohydrate moiety on the stability of glycoproteins. *Biochemistry* **35:** 7299–7307.

Weston, S.A., Tucker, A.D., Thatcher, D.R., Derbyshire, D.J., and Pauptitl, R.A. 1994. X-ray structure of recombinant ricin A chain at 1.8 Å resolution. *J. Mol. Biol.* **244:** 410–422.